Estimating Soil Moisture Conditions of the Greater Changbai Mountains by Land Surface Temperature and NDVI

Yang Han, Yeqiao Wang, and Yunsheng Zhao

***Abstract*—Soil moisture is an important indicator of the land surface environment. The combination of land surface temperature (LST) and normalized difference vegetation index (NDVI) could enhance the ability of extracting information on soil moisture conditions. In this study, we employed multitemporal Moderate Resolution Imaging Spectroradiometer (MODIS) data products of LST, NDVI, and land cover types to obtain the information about soil moisture for the greater Changbai Mountains. We selected nine time periods in 2007 for inversion of the soil moisture conditions and focused the analysis on four critical time periods. According to the spatial pattern of the LST and NDVI, we established the "wet-edge" and "dry-edge" equations and determined the relative parameters. We obtained the temperature–vegetation dryness index (TVDI) using the wet-edge and dry-edge relationships to reveal temporal changes of the land surface soil moisture conditions of the study area. We also analyzed the relationship between different land cover types in five TVDI classes. This paper demonstrates that TVDI is an effective indicator to detect soil moisture status in the greater Changbai Mountains region.**

***Index Terms*—Changbai Mountains, land surface temperature (LST), Moderate Resolution Imaging Spectroradiometer (MODIS), normalized difference vegetation index (NDVI), temperature–vegetation dryness index (TVDI).**

I. Introduction

SOIL moisture is one of the most important land environmental variables relative to land surface climatology, hydrology, and ecology [1]. Soil moisture conditions play a critical role in evaluating terrestrial ecological environmental conditions and atmospheric processes [2]. Variations in soil moisture produce significant changes in surface energy balance, regional runoff, and vegetation productivity. Accurate assessment of such a variable is difficult both because typical field methods are complex and expensive and local-scale variations in soil properties, terrain, and vegetation cover make selection of representative field sites difficult, if not impossible [3]. The most important potential application of land surface moisture is to provide information for agricultural practice and management decisions [4], in particular, in water-stressed regions. Spatially distributed land surface moisture estimation is usually based on interpolation of data or modeling of environmental factors such as climate, land use, soil, temperature, and vegetation. Soil moisture is one of the important parameters for ecosystem modeling, simulation, and predictions [5], and recent applications of remote sensing to soil moisture assessment have suggested that good measurement approaches provide more efficient and effective results. Many models have been developed to retrieve soil moisture conditions (e.g., [6]–[11]).

Reported studies have employed remotely sensed data for obtaining land surface conditions. The mostly used indexes are the normalized difference vegetation index (NDVI), land surface temperature (LST), the soil-adjusted vegetation index (SAVI), and the modified SAVI. Those indexes have been used to estimate changes in vegetation, surface-soil moisture, and evapotranspiration. NDVI is considered as a conservative indicator of water stress because vegetation remains green after initial water stress. In contrast, the surface temperature can rise rapidly with water stress [12]. LST is an important indicator of conservation of balance and greenhouse effects. It is a key factor in the geophysical process of regional and global scales [13]. It is also an important parameter to control the biogeophysical and biogeochemical processes, particularly for meteorological and climatological studies [14], [15]. Vegetation coverage and surface temperature are important parameters in describing the characteristics of landscape features which, in combination, can provide information on vegetation and soil moisture conditions at the surface [16]. While NDVI reflects the conditions of vegetation and land cover information, LST reflects the status of soil moistures. Information of NDVI and LST complements each other, and the relationship from the two offers the potential to monitor soil moisture [17]. The reported studies exploring such relationships can be grouped into three broad aspects.

1) The LST/NDVI combination (e.g., [18] and [19]) typically shows a strong negative relationship ($R^2 = 0.92$). The slope of the LST/NDVI relationship has an indication

Manuscript received April 6, 2009; revised July 8, 2009. Date of publication March 8, 2010; date of current version May 19, 2010. This work was supported in part by the Natural Science Foundation of China (40971190, 40771153), by the Science and Technology Innovation Foundation of Northeast Normal University (106111065202), by the National Grand Fundamental Research 973 Program of China (2009CB426305), by the Fundamental Research Funds for the Central Universities (09SSXT130), and by the China Scholarship Council.

Y. Han and Y. Wang are with the College of Urban and Environmental Science, Northeast Normal University, Changchun 130024, China, and also with the Department of Natural Science, University of Rhode Island, Kingston, RI 02881 USA (e-mail: hany025@hotmail.com; yqwang@uri.edu).

Y. Zhao is with the College of Urban and Environmental Science, Northeast Normal University, Changchun 130024, China (e-mail: zhaoys975@nenu.edu.cn).

Color versions of one or more of the figures in this paper are available online at http://ieeexplore.ieee.org.

Digital Object Identifier 10.1109/TGRS.2010.2040830

0196-2892/$26.00 © 2010 IEEE

of the "wetness" of the land surface. It provides information, such as stomatal resistance and evapotranspiration, at the intrinsic surface (e.g., deciduous forest), which is sensitive to surface-moisture conditions. Nemani *et al.* [20] extracted the slope of the LST/NDVI relationship in different places from the same image and found that it could reflect soil moisture status. Analysis of the LST/NDVI has also been used to assess information related to area-averaged soil moisture conditions. By calculating the parameters by the LST/NDVI relationship, we could extract soil moisture information in different places and temporal changes. Therefore, it has been used for soil moisture inversion of large areas.

2) Moran *et al.* [21] extended the LST/NDVI method to develop a soil-canopy water deficit index (WDI) using information in the LST/NDVI space. The WDI was originally derived from the concept of crop water stress index. This approach used a "vegetation index temperature trapezoid" and was based on the hypothesis that a trapezoidal shape would result from a plot of the difference between observed surface and air temperatures at the intrinsic surface if there is sufficient variation of fractional vegetation cover and surface water conditions. For this approach, a range of vegetation cover and soil water content was a critical factor in determining the shape of the trapezoid, and thus, the relationship was demonstrated.
3) Following [21], Sandholt *et al.* [22] developed a temperature–vegetation dryness index (TVDI). The TVDI was obtained using advanced very high resolution radiometer and the derivatives of LST and NDVI. The TVDI approach was applied in a region that has mixed land covers of dry grasslands, shrub lands, and cultivated areas and related the land cover types to soil moisture status. A scatter plot of remotely sensed surface temperature and NDVI was assumed to take a triangular shape. TVDI could be estimated from the dry and wet edges of a triangle. TVDI could depend on the graph data by calculation of the vegetation index and the surface temperature. It is simple and convenient to calculate TVDI and directly obtain the modeling parameters from the characteristic of reversing the soil moisture. Nishida *et al.* [23] developed an estimation method of evapotranspiration index for monitoring the surface-moisture status and tested the algorithm using Moderate Resolution Imaging Spectroradiometer (MODIS) data sets from the year 2000. Another study [24] described the "triangle" method for estimating the soil moisture wetness and evapotranspiration fraction from satellite imagery and illustrated how the triangle could be created from a land surface model.

The MODIS data products have advantages in tripartite high spatial, temporal, and spectral resolutions. MODIS data products include NDVI and LST [25] that make the derivation of soil moisture conditions for a large regional scale monitoring possible. The combination of the MODIS data products offer readily available LST and NDVI data for extraction of soil moisture information, in particular, for regional and global scale ecosystem characterizations [26].

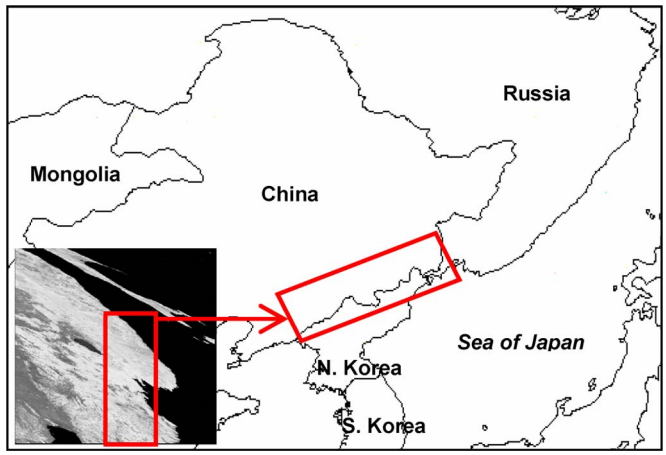

Fig. 1. Study area of the greater Changbai Mountains.

In this paper, we used the MODIS data products of LST, NDVI, and land cover types to estimate the spatial and temporal changes of soil moisture status and water conditions in the greater Changbai Mountains of Northeast China, which reflected the topographic and terrain effects. This paper explores one such "combined" method (combination of NDVI and LST) TVDI approach, which has an advantage over other indexes (such as the LST/NDVI curve) in that it can be applied to mixed land surfaces, and derives surface-moisture status from satellite information. The approach of TVDI could analyze a spatial or contextual array of remotely sensed spectral solar-reflective and thermal-infrared measurements to estimate near-surface soil moisture conditions. We used the TVDI concept to understand the relationship between NDVI and LST and grouped TVDI into different classes according to spatiotemporal distribution characteristics.

II. Materials and Methods

A. Study Area

The study area is the greater Changbai Mountains (Fig. 1), centered at $(128°3'12''\ \mathrm{E}, 42°0'36''\ \mathrm{N})$ in Northeast China. The study area includes part of the northeast provinces of Heilongjiang, Jilin, and Liaoning in China, the north provinces of Ryannggang and Chagang of North Korea, and a portion of the Russian Far East. Geologically, the region is situated at the edge of the East Asia continent on the border of the Pacific competent zone. It covers 248 000 km^2 of mountains terrain. The highest elevation is 2749 m above sea level. The peak of the Changbai Mountains is the head of three major rivers of Songhua, Yalu, and Tumen. Among those, the Yalu and Tumen are the border rivers between China and North Korea. The Himalayan tectonic movement since the Miocene Epoch had resulted in volcanic eruptions and hence, the formation of a typical volcanic geomorphological region composed of volcanic cones, inclined plateau, and lava tablelands. Recent small-scale volcano eruptions occurred in 1597, 1668, and 1702 and a very large scale eruption occurred during 1100–1410 [27], [28].

Situated in this region, the Changai Mountain Natural Reserve has the largest protected temperate forest in Northeast Asia. It is the home to endangered Siberian tigers and the last stands of virgin Korean pine-mixed hardwood [29]. The climate is characterized by cold weather during long winter and short cool summers. The annual mean temperature in the study area ranges from $-7\,^{\circ}$C to $3\,^{\circ}$C, and the annual average precipitation ranges from 400 to 1400 mm [30]. The climate and terrain conditions support four vertically distributed vegetation zones including, from bottom to top, needle and broad-leaved mixed forests (below 1000 m); old-growth mixed broadleaf Korean pine (*Pinus koraiensis*) forests (1100–1800 m); dwarf-birch (*Betula ermanii*) forests (1800–2100 m); and Alpine tundra (above 2100 m). This natural reserve and the surrounding areas have been a research focus in ecosystem and biodiversities and with remote sensing applications [31].

B. Data Source

The three types of MODIS data products included the eight-day composite land surface temperature (MOD11A2) of 2007, the 16-day composite ground vegetation index (MOD13A2) of 2007, and land cover types (MOD12Q2) between 2001 and 2004. We processed the two temporal-phase eight-day composite LST data to match up with a single temporal-phase 16-day composite NDVI image. For the MOD12Q2 data set, we adopted the International Geosphere–Biosphere Programme (IGBP) global vegetation classification scheme for the purpose of this study. The major land cover types include water, evergreen needleleaf forest, evergreen broadleaf forest, deciduous needleleaf forest, deciduous broadleaf forest, mixed forests, shrublands, woody savannas, grasslands, permanent wetlands, crop land, urban and buildup, permanent snow and ice, and barren or sparsely vegetated land. For the purpose of this study, we focused on water, mixed forest, crop land, urban and buildup, and deciduous broadleaf forest. The spatial resolution of the aforementioned data sets is 1 km in all. We selected nine time periods of MODIS NDVI and LST data products, one period per month from March to November in 2007, and performed data preprocessing accordingly. As the MOD12Q2 is not available for the year 2007 and we considered that the areas of changed land cover types between 2004 and 2007 in the greater Changbai Mountains region are negligible for monitoring the soil moisture condition, we chose to use the MOD12Q2 of 2004 for quantification of the ratios of land cover types in derivation of the TVDI in 2007.

C. TVDI

NDVI provides information about the growing states and conditions of vegetation on the ground. Land surface temperature reflects certain state of soil moisture. The combination of the two can establish a potential relationship to reveal land surface moisture. The LST/NDVI relationship [32] typically shows a strong negative relationship between surface temperature and the spectral vegetation index [33]. The studies [22] developed a simplified land surface dryness index, i.e., TVDI. In this approach, a scatter plot of remotely sensed LST and NDVI was assumed to take a triangular shape, and the TVDI could be estimated from the dry and wet edges of the triangle (Fig. 2).

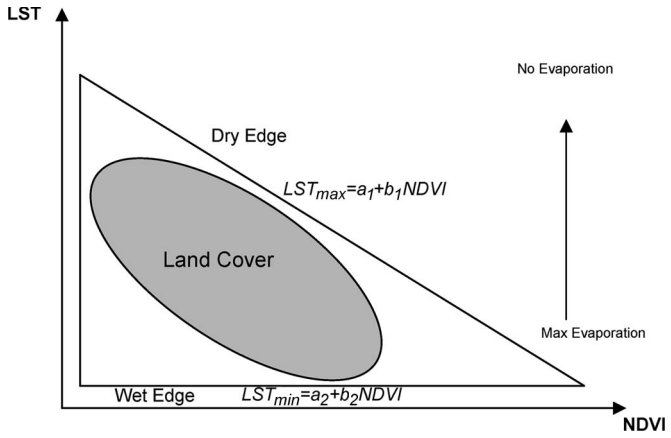

Fig. 2. Simplified LST-NDVI triangle space (adapted from [14]).

TABLE I
EQUATIONS OF WET EDGE AND DRY EDGE AND THE PARAMETERS

Date	LST_{max} *(K)*	LST_{min} *(K)*
March	LST_{max}=271-9.4404NDVI R^2=0.9691	LST_{min}=265.37+1.3053NDVI R^2=0.7238
June	LST_{max}=318-25.331NDVI R^2=0.931	LST_{min}=297.85-7.6876NDVI R^2=0.8469
August	LST_{max}=307.48-10.292NDVI R^2=0.8082	LST_{min}=301.9-11.384NDVI R^2=0.8791
November	LST_{max}=292.03-20.855NDVI R^2=0.9283	LST_{max}=280.79+1.712NDVI R^2=0.8104

In the feature space, we processed the information about the wet edge ($\mathrm{LST_{min}}$, maximum evapotranspiration and thereby, unlimited water access) as a straight line parallel with NDVI axes. The dry edge ($\mathrm{LST_{max}}$, limited water availability) is linearly correlated with NDVI (Fig. 2). We calculated the TVDI value ranging from zero to one for each pixel of image based on its position in the feature space. TVDI values of one at the dry edge correspond to limited water availability, and zero at the wet edge correspond to maximum evapotranspiration and thereby, unlimited water access. The higher the TVDI value, the lower the soil moisture content is. TVDI is defined as

$$\mathrm{TVDI} = \frac{\mathrm{LST} - \mathrm{LST_{min}}}{\mathrm{LST_{max}} - \mathrm{LST_{min}}} \tag{1}$$

where

$$\mathrm{LST_{max}} = a_1 + b_1 \times \mathrm{NDVI} \tag{2}$$

$$\mathrm{LST_{min}} = a_2 + b_2 \times \mathrm{NDVI} \tag{3}$$

where LST is the observed surface temperature (K or $^{\circ}$C) at a given pixel. $\mathrm{LST_{max}}$ is the maximum surface temperature observation for a given NDVI and a_1 and b_1 define the dry edge as a linear fit to the data; a_2 and b_2 define the wet edge, which is the minimum surface temperature in the triangle. Theoretically,

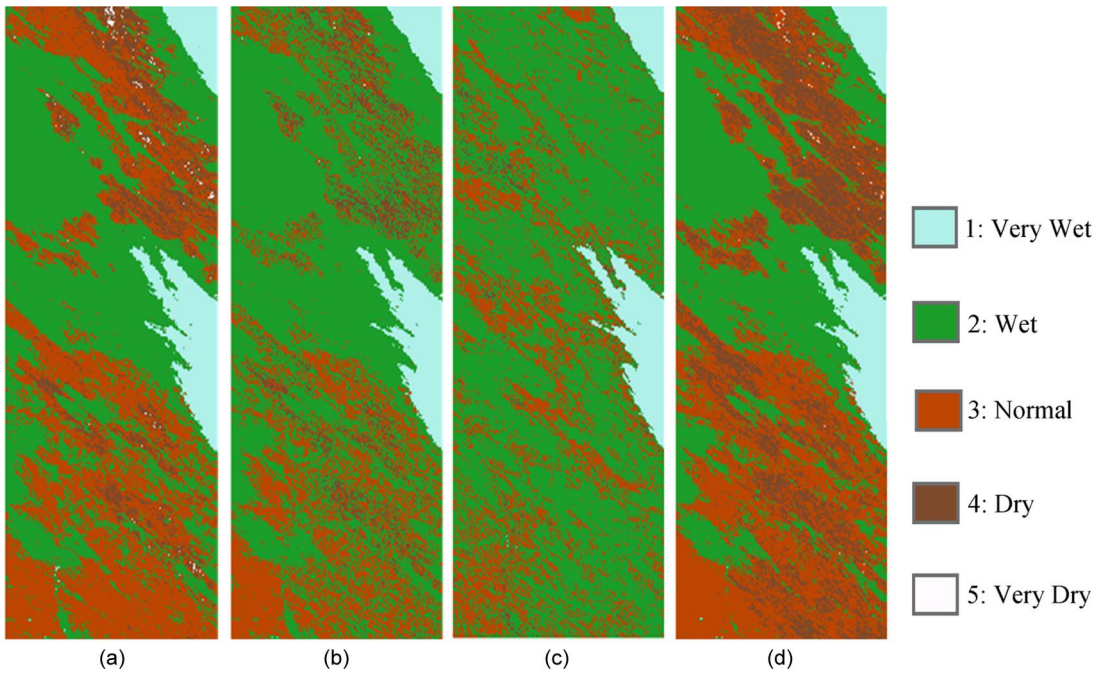

Fig. 3. Classification of the four typical periods by TVDI. (a) March. (b) June. (c) August. (d) November.

in the feature space of NDVI and LST, the dry edge represents pixels valued at zero, and the wet edge represents pixels valued at 100% of the relative soil moisture. Therefore, TVDI could be represented by relative soil moisture value in the images, and we can compare the relative soil moisture values with different times and different images. The uncertainty of TVDI is larger for high NDVI values, where the TVDI isolines are closely set.

III. Results and Discussions

A. Relationship Between LST and NDVI

We estimated the parameters of a_1, b_1, a_2, and b_2 on the basis of pixel values from the study area. In order to determine the parameters, we calculated the linear regressions on the dry edge and wet edge in the LST/NDVI space.

We selected four typical months of March, June, August, and November in 2007 for discussions (Table I). The functions of LST and NDVI for each time period illustrated the seasonal variability of the parameters. In the greater Changbai Mountain region, March could be characterized by low NDVI and low LST. The dry-edge position relationship has a high correlation coefficient $R^2 > 0.95$, and the wet-edge position relationship has a correlation coefficient $R^2 > 0.7$. The relationship showed that LST was higher in the areas with more vegetation cover in this time period. In June, the NDVI and the LST increased as the vegetation cover was changing rapidly. There was a negative relationship between LST $(\mathrm{LST}_{\max}, \mathrm{LST}_{\min})$ and NDVI, with correlation coefficients $R^2 > 0.93$ in wet condition and $R^2 > 0.84$ in dry condition. From June to August, the LST increased, while NDVI remained almost unchanged. During this time period, the wet-edge linear equation has a correlation coefficient $R^2 > 0.8$ and the dry-edge linear equation has a correlation coefficient $R^2 > 0.87$. In November both LST and NDVI had decreased with correlation coefficient $R^2 > 0.92$ in dry edge and correlation coefficient $R^2 > 0.81$ in wet edge. The variations in different seasons show that both NDVI and LST rise first and then decline. It indicates that when the soil moisture is high, the absorption of solar energy is mainly consumed for evaporation, and the difference of the soil and canopy temperatures is not obvious. When the soil moisture content is low, the bare soil surface are drying rapidly, and the evaporation is small and absorption is mainly used in solar surface temperature. When the soil-surface temperature is high, the moisture in the root layer of vegetation is consumed to maintain a high transpiration rate. The relationship between LST and NDVI reflects the state of the regional soil moisture.

B. Temporal and Spatial Evolution of TVDI

Compared with the space characteristics of NDVI and LST, we used (1) to calculate the TVDI of pixels by the equations of dry edge and wet edge. We classified the soil moisture for five categories, i.e., 1) very wet $(0 < \mathrm{TVDI} < 0.1)$; 2) wet $(0.1 < \mathrm{TVDI} < 0.4)$; 3) normal $(0.4 < \mathrm{TVDI} < 0.6)$; 4) dry $(0.6 < \mathrm{TVDI} < 0.9)$; and 5) very dry $(0.9 < \mathrm{TVDI} < 1)$. Fig. 3 shows the spatial distribution of TVDI for March, June, August, and November in 2007, respectively. The seasonal variations in TVDI are observable from Fig. 4. The areas of ocean surface, for example, have the lowest TVDI (valued at zero).

Fig. 4 shows the comparison of the mean and variance of TVDI in the study area. The seasonal variations of TVDI in different months in 2007 are evident. The mean TVDI of the area was lowest $(m < 0.2)$ in August due to the relatively high surface temperature of the different land cover types. In the months of March, June, and November, the mean TVDI increased, and there was little change in the variance. In the study area, when precipitation is abundant, particularly in rainy

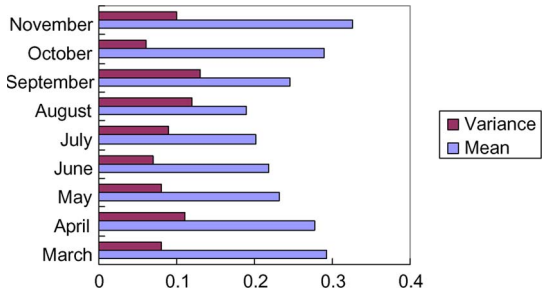

Fig. 4. Mean and variance of TVDI in the greater Changbai Mountain regions.

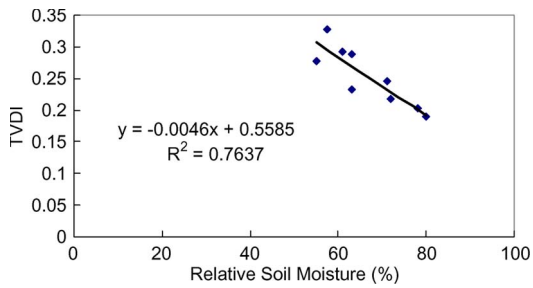

Fig. 5. Relationship between TVDI and the relative soil moisture.

season, the evaporation capacity of the vegetation canopy is large, and the surface temperature is correspondingly high; NDVI, which reflects the livingness of vegetation, is high as well. Similarly, when the surface temperature is low and vegetation cannot obtain enough water supplies, the evaporation capacity of the vegetation canopy is small, and the NDVI value is low. Therefore, TVDI reflects the surface moisture status and the vegetation capacity.

C. Comparing TVDI and Detecting Moisture

In general, TVDI is sensitive to rainfall and decreases after rain events. To illustrate the differences of wetness and drought conditions in overall magnitude and the differences in seasonal variations, we made a comparison between TVDI and *in situ* measurements of relative soil moisture data collected from the observatory station in Changbai Mountain area. The data of relative soil moisture were obtained from different observatory stations in the study area in 2007. Because the observatory stations are distributed evenly in the study area, we used the mean of the relative soil moistures collected from different observatory stations every month and made a comparison between the mean TVDI we got every month and the mean of relative soil moistures every month. It is a good demonstration that TVDI can reflect the soil moisture in the greater Changbai Mountains area. TVDI values are plotted as function of soil moisture (Fig. 5). The relationship shows that higher soil moisture values correspond to lower TVDI values. Linear relationships exist between TVDI and the relative soil moisture with $R^2 > 0.70$.

D. Comparing TVDI and Land Cover Types

In order to understand the relationship between TVDI and land cover types in the Changbai Mountains area, we obtained the map of land cover type data in the year 2004 by classification of MOD12Q2 data (Fig. 6). To illustrate soil moisture-condition differences in seasonal response, we performed a classification based on temporal and spatial patterns of TVDI. We then calculated the percentage of the land cover types of water, mixed forest, urban and buildup, cropland, and deciduous broadleaf forest corresponding to the five TVDI classes by an aggregation process (Fig. 7). We performed the different land cover type extraction for each TVDI class, which reflected the spatial trend of land surface soil moisture conditions.

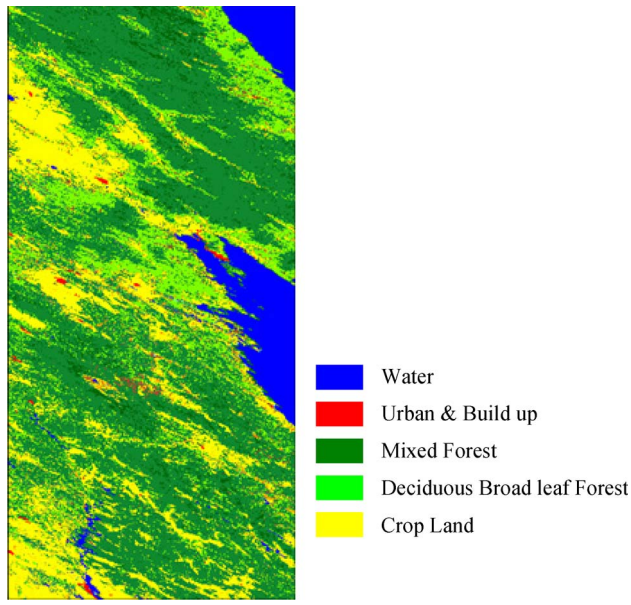

Fig. 6. Map of different land cover types.

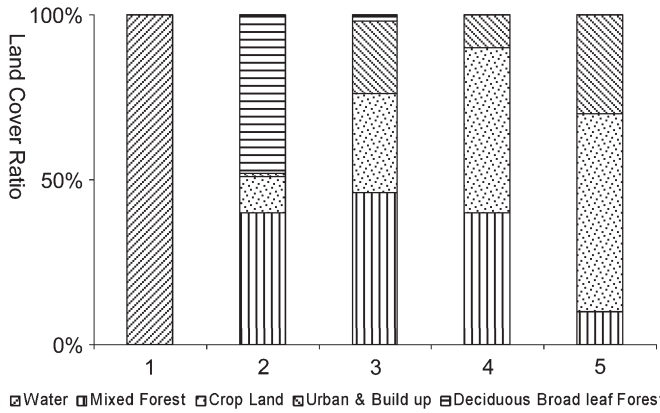

Fig. 7. Land cover types in five different TVDI class.

The comparisons indicate that TVDI class 1 is for very wet condition such as water bodies. TVDI class 2 contains four land cover types of mixed forest, urban and buildup, cropland, and deciduous broadleaf forest. The ratios between mixed forest and deciduous broadleaf forest are high, and urban and buildup are low. For class 3 to class 5, the percentages of mixed forest decreased and those of the cropland increased. We could infer that moisture condition in forest area was better than that of cropland and urban land in wet conditions from the aforementioned result.

IV. Conclusion

The combination of NDVI and LST from MODIS data products is a useful tool for studying soil moisture. The LST and NDVI document substantial change of land surface characteristics between wet and dry days over the greater Changbai Mountain region. The time series of NDVI, LST, and the derivative of TVDI revealed spatiotemporal characteristics of soil moisture conditions. The results show that the combination of LST and NDVI can enhance the ability of extracting the soil moisture conditions for a large area and in high time frequency. The parameters reflect the surface-soil moisture status and achieve a good match up with field-collected relative soil moisture $(R^2 > 0.70)$. The seasonal variations indicate that the trend in TVDI is lower in the rainy season in the study area. Typically, in August, the variance of NDVI reached a minimum. In addition, using time-series MODIS data products, we can determine the relationships between TVDI and land cover types. An improved land cover classification result may help derive moisture information according to the vegetation characteristics of each land cover type.

The results have demonstrated the advantages of extracting soil moisture condition by remotely sensed data. LST and NDVI are correlated to moisture availability in a large spatial scale. The possibility of inferring surface-moisture conditions from regular remote sensing data products helps significantly in the understanding and monitoring of the ecosystem conditions and the environment.

Acknowledgment

The Institute of Geographic Sciences and Natural Resources Research of the Chinese Academy of science provided the soil data.

References

[1] P. J. Sellers and D. S. Schimel, "Remote sensing of the land biosphere and biogeochemistry in the EOS era: Science priorities, methods and implementation," *Global Planetary Change*, vol. 7, no. 4, pp. 279–297, 1993.

[2] K. Song, X. Zhou, and Y. Fan, "Empirically adopted IEM for retrieval of soil moisture from radar backscattering coefficients," *IEEE Trans. Geosci. Remote Sens.*, vol. 47, no. 6, pp. 1662–1672, Jun. 2009.

[3] S. N. Goward, Y. Xue, and K. P. Czajkowski, "Evaluating land surface moisture conditions from the remotely sensed temperature/vegetation index measure: An exploration with the simplified biosphere model," *Remote Sens. Environ.*, vol. 79, no. 2/3, pp. 225–242, Feb. 2002.

[4] J. Penuelas, I. Filella, C. Biel, L. Serrano, and R. Save, "The reflectance at the 950–970 mm region as an indicator of plant water status," *Int. J. Remote Sens.*, vol. 14, no. 10, pp. 1887–1905, Jul. 1993.

[5] R. Nemani, H. Hashimoto, P. Votava, F. Melton, W. Wang, A. Michaelis, L. Mutch, C. Milesi, S. Hiatt, and M. White, "Monitoring and forecasting ecosystem dynamics using the Terrestrial Observation and Prediction System (TOPS)," *Remote Sens. Environ.*, vol. 113, no. 7, pp. 1497–1509, Jul. 2009.

[6] C. Notarnicola, M. Angiulli, and F. Posa, "Soil moisture retrieval from remotely sensed data: Neural network approach versus Bayesian method," *IEEE Trans. Geosci. Remote Sens.*, vol. 46, no. 2, pp. 547–557, Feb. 2008.

[7] M. Aribi, C. Andre, and B. Decharme, "A method for soil moisture estimation in western Africa based on the ERS scatterometer," *IEEE Trans. Geosci. Remote Sens.*, vol. 46, no. 2, pp. 438–448, Feb. 2008.

[8] M. Moghaddam, Y. Rahmat-samii, E. Rodriguez, D. Entekhabi, J. Hoffman, D. Moller, L. E. Pierce, S. Saatchi, and M. Thomson, "Microwave observatory of subcanopy and subsurface (MOSS): A mission concept for global deep soil moisture observations," *IEEE Trans. Geosci. Remote Sens.*, vol. 45, no. 8, pp. 2630–2643, Aug. 2007.

[9] C. H. Kuo and M. Moghaddam, "Electromagnetic scattering from multilayer rough surfaces with arbitrary dielectric profiles for remote sensing of subsurface soil moisture," *IEEE Trans. Geosci. Remote Sens.*, vol. 45, no. 2, pp. 349–366, Feb. 2007.

[10] S. C. Dunne, D. Entekhabi, and E. G. Njoku, "Impact of multiresolution active and passive microwave measurements on soil moisture estimation using the ensemble Kalman smoother," *IEEE Trans. Geosci. Remote Sens.*, vol. 45, no. 4, pp. 1016–1028, Apr. 2007.

[11] N. E. C. Verhoest, B. de Baets, and H. Vernieuwe, "A Takagi–Sugeno fuzzy rule-based model for soil moisture retrieval from SAR under soil roughness uncertainty," *IEEE Trans. Geosci. Remote Sens.*, vol. 45, no. 5, pp. 1351–1360, May 2007.

[12] S. J. Goetz, "Multisensor analysis of NDVI, surface temperature and biophysical variables at a mixed grassland site," *Int. J. Remote Sens.*, vol. 18, no. 1, pp. 71–94, Jan. 1997.

[13] Z. Wan, "New refinements and validation of the MODIS land-surface temperature/emissivity products," *Remote Sens. Environ.*, vol. 112, no. 1, pp. 59–74, Jan. 2008.

[14] C. Coll, S. J. Hook, and J. M. Galve, "Land surface temperature from the Advanced Along-Track Scanning Radiometer: Validation over inland waters and vegetated surface," *IEEE Trans. Geosci. Remote Sens.*, vol. 47, no. 1, pp. 350–360, Jan. 2009.

[15] J. M. Galve, C. Coll, V. Caselles, and E. Valor, "An atmospheric radiosounding database for generating land surface temperature algorithms," *IEEE Trans. Geosci. Remote Sens.*, vol. 46, no. 5, pp. 1547–1557, May 2008.

[16] Z. G. Li, Y. L. Wang, Q. B. Zhou, J. S. Wu, J. Peng, and H. Chang, "Spatiotemporal variability of land surface moisture based on vegetation and temperature characteristics in Northern Shaanxi Loess Plateau, China," *J. Arid Environ.*, vol. 72, no. 6, pp. 974–985, Jun. 2008.

[17] D. Luquet, A. Vidal, J. Dauzat, A. Begue, A. Olioso, and P. Clouvel, "Using directional TIR measurements and 3D simulations to assess the limitations and opportunities of water stress indices," *Remote Sens. Environ*, vol. 90, no. 1, pp. 53–62, Mar. 2004.

[18] S. N. Goward, G. D. Cruickhanks, and A. S. Hope, "Observed relation between thermal emission and reflected spectral radiance of a complex vegetated landscape," *Remote Sens. Environ.*, vol. 18, no. 2, pp. 137–146, Oct. 1985.

[19] R. R. Nemani and S. W. Running, "Estimation of regional surface resistance to evapotranspiration from NDVI and thermal IR AVHRR data," *J. Appl. Meteorol.*, vol. 28, no. 4, pp. 276–284, Apr. 1989.

[20] R. R. Nemani, L. Pierce, S. W. Running, and S. N. Goward, "Developing satellite-derived estimates of surface moisture status," *J. Appl. Meteorol.*, vol. 32, no. 3, pp. 548–557, Mar. 1993.

[21] M. S. Moran, T. R. Clarke, Y. Inoue, and A. Vidal, "Estimating crop water deficit using the relation between surface-air temperature and spectral vegetation index," *Remote Sens. Environ.*, vol. 49, no. 3, pp. 246–263, Sep. 1994.

[22] I. Sandholt, K. Rasmussena, and J. Andersenb, "A simple interpretation of the surface temperature/vegetation index space for assessment of surface moisture status," *Remote Sens. Environ.*, vol. 79, no. 2/3, pp. 213–224, Feb. 2002.

[23] K. Nishida, R. R. Nemani, J. M. Glassy, and S. W. Running, "Development of an evapotranspiration index from Aqua/MODIS for monitoring surface moisture status," *IEEE Trans. Geosci. Remote Sens.*, vol. 41, no. 2, pp. 453–501, Feb. 2003.

[24] T. Carlson, "An overview of the 'Triangle method' for estimating surface evapotranspiration and soil moisture from satellite imagery," *Sensors*, vol. 7, no. 8, pp. 1612–1629, 2007.

[25] Z. Wan, P. Wang, and X. Li, "Using MODIS land surface temperature and normalized difference vegetation index for monitoring drought in the southern Great Plains, USA," *Int. J. Remote Sens.*, vol. 25, no. 1, pp. 61–72, Jan. 2004.

[26] C. O. Justice, E. Vermote, J. Townshend, R. Defries, D. P. Roy, D. K. Hall, V. V. Salomonson, J. L. Privette, G. Riggs, A. Strahler, W. Lucht, R. B. Myneni, Y. Knyazikhin, S. W. Running, R. R. Nemani, Z. M. Wan, A. R. Huete, W. Leeuwen, R. E. Wolfe, L. Giglio, J. P. Muller, P. Lewis, and M. J. Barnsley, "The Moderate Resolution Imaging Spectroradiometer (MODIS): Land remote sensing for global change research," *IEEE Trans. Geosci. Remote Sens.*, vol. 36, no. 4, pp. 1228–1249, Jul. 1998.

[27] D. C. Zhao, "Preliminary study of the effects of volcano on vegetation development and succession," (in Chinese), *For. Ecosyst. Res.*, vol. 2, pp. 81–87, 1981.

[28] Q. Liu, Z. Wang, and S. Wang, "Recent volcano eruptions and vegetation history of alpine and sub-alpine of Changbai Mountain," (in Chinese), *For. Ecosyst. Res.*, vol. 6, pp. 57–62, 1992.

[29] R. Stone, "A threatened nature reserve breaks down Asian borders," *Science*, vol. 313, no. 5792, pp. 1379–1380, Sep. 2006.
[30] X. Chen and B. Li, "Change in soil carbon and nutrient storage after human disturbance of a primary Korean pine forest in Northeast China," *For. Ecol. Manag.*, vol. 186, no. 1–3, pp. 197–206, 2003.
[31] Q. J. Liu, X. R. Li, Z. Q. Ma, and N. Takeuchi, "Monitoring forest dynamics using satellite imagery—A case study in the natural reserve of Changbai Mountain in China," *For. Ecol. Manag.*, vol. 210, no. 1–3, pp. 25–37, May 2005.
[32] S. N. Goward, G. D. Cruickhanks, and A. S. Hope, "Observed relation between thermal emission and reflected spectral radiance of a complex vegetated landscape," *Remote Sens. Environ.*, vol. 18, no. 2, pp. 137–146, Oct. 1985.
[33] R. R. Gillies, W. P. Kustas, and K. S. Humes, "A verification of the "triangle" method for obtaining surface soil water content and energy fluxes from remote measurements of the Normalized Difference Vegetation Index (NDVI) and surface radiant temperature," *Int. J. Remote Sens.*, vol. 18, no. 15, pp. 3145–3166, Oct. 1997.

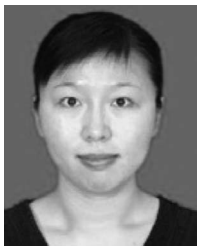

Yang Han received the B.S. degree from the College of Urban and Environmental Science, Northeast Normal University, Changchun, China, in 2006, where she is currently working toward the Ph.D. degree in remote sensing.

She is also currently a Visiting Student at the Department of Natural Resource Science, University of Rhode Island, Kingston. Her research interests are in the field of terrestrial remote sensing and quantitative remote sensing.

Yeqiao Wang received the Ph.D. degree from the University of Connecticut, Storrs, in 1995.

He is currently a Professor in terrestrial remote sensing with the Department of Natural Resource Science, University of Rhode Island, Kingston. His research interests are in natural resources and environmental modeling.

Yunsheng Zhao received the B.S. degree in mathematics from Northeast Normal University, Changchun, China, in 1975.

He is currently a Professor in remote sensing with the College of Urban and Environmental Science, Northeast Normal University. His main research activities are in quantitative remote sensing and their applications.